Constant-Wall-Temperature Nusselt Number in Micro and Nano-Channels[1]

Nicolas G. Hadjiconstantinou

Olga Simek

Mechanical Engineering Department,
Massachusetts Institute of Technology,
Cambridge, MA 02139

We investigate the constant-wall-temperature convective heat-transfer characteristics of a model gaseous flow in two-dimensional micro and nano-channels under hydrodynamically and thermally fully developed conditions. Our investigation covers both the slip-flow regime $0 \leqslant Kn \leqslant 0.1$, and most of the transition regime $0.1 < Kn \leqslant 10$, where Kn, the Knudsen number, is defined as the ratio between the molecular mean free path and the channel height. We use slip-flow theory in the presence of axial heat conduction to calculate the Nusselt number in the range $0 \leqslant Kn \leqslant 0.2$, and a stochastic molecular simulation technique known as the direct simulation Monte Carlo (DSMC) to calculate the Nusselt number in the range $0.02 < Kn < 2$. Inclusion of the effects of axial heat conduction in the continuum model is necessary since small-scale internal flows are typically characterized by finite Peclet numbers. Our results show that the slip-flow prediction is in good agreement with the DSMC results for $Kn \leqslant 0.1$, but also remains a good approximation beyond its expected range of applicability. We also show that the Nusselt number decreases monotonically with increasing Knudsen number in the fully accommodating case, both in the slip-flow and transition regimes. In the slip-flow regime, axial heat conduction is found to increase the Nusselt number; this effect is largest at $Kn = 0$ and is of the order of 10 percent. Qualitatively similar results are obtained for slip-flow heat transfer in circular tubes. [DOI: 10.1115/1.1447931]

Keywords: Heat Transfer, Microscale, Molecular Dynamics, Monte Carlo, Nanoscale

1 Introduction

Over the last decade there has been an enormous interest in micro and nano-technology. As systems approach microscopic scales, increasing deviations from the well-established continuum laws are reported [17]. In dilute gaseous flows the failure of the continuum description is quantified by the Knudsen number, defined here as the ratio of the molecular mean free path λ to the channel height H. The regime $0 \leqslant Kn \leqslant 0.1$ is referred to as slip-flow; no-slip is captured by $Kn = 0$. For $Kn \gtrsim 0.1$ the continuum description is expected to fail [7], and the regime $0.1 < Kn \leqslant 10$ is referred to as the transition regime because the molecular motion undergoes a transition from diffusive (continuum) for $Kn \lesssim 0.1$, to ballistic for $Kn \gtrsim 10$ (free molecular flow).

In this paper we consider the constant-wall-temperature heat-transfer characteristics of two-dimensional channels that are sufficiently long for flow to be fully developed. Our objective is to understand convective heat transfer in the transition regime, and in particular, to bridge the continuum slip-flow physics to the transition-regime physics. This is a difficult task; the flow physics includes the effects of compressibility, viscous heating, expansion cooling, and thermal creep, which are typically neglected in continuum analyses. For the above reasons, we have performed our molecular simulations on a model problem that requires minimal modeling on the simulation side such that critical comparison between continuum and molecular solutions can be directly translated into information about the validity of the continuum model that is ultimately the most convenient modeling tool. Our model problem focuses on monoatomic gases that do not require modeling of the rotational energy exchange; the latter will be undertaken in a future study. For reasons of computational convenience we have used the simplest monoatomic gas model, the hard sphere gas; similarity guarantees that our non-dimensional results are valid for all dilute monoatomic gases. Our continuum solutions are, of course, not specific to monoatomic gases; this will be further discussed below. Our molecular simulations were performed using a stochastic simulation technique known as the direct simulation Monte Carlo (DSMC).

The constant-wall-temperature Nusselt number in the slip-flow regime can be determined using continuum theory subject to slip boundary conditions (both velocity and temperature); this was first undertaken by Inman [18]. The work of Inman shows that for fully accommodating walls the Nusselt number decreases in the presence of slip, as expected. This was verified by Kavehpour et al. [19], who performed a series of continuum calculations in the slip-flow regime investigating the relative effects of rarefaction and compressibility. However, the work of Inman and subsequent investigators did not include the effects of axial heat conduction that become important for low Peclet numbers that are typical in small scale geometries.

The effects of axial heat conduction have only been investigated in the no-slip limit. The original investigation by Pahor and Strnad [29] shows that in the presence of axial heat conduction the Nusselt number monotonically increases, approaching the limiting value $Nu_T = 8.1174$ as the Peclet number goes to zero. This represents an increase of approximately 10 percent compared to the typically studied infinite Peclet number limit ($Nu_T = 7.5407$).

The constant-wall-temperature convective heat-transfer characteristics of gaseous internal flows in the transition regime are not known. Hadjiconstantinou [13] performed direct Monte Carlo simulations to show that in the constant-wall-heat-flux case the Nusselt number decreases monotonically with increasing rarefaction (Kn) in the fully accommodating case.

The use of the direct simulation Monte Carlo method for modeling flows in microdevices was introduced by Piekos and Breuer [30] and Alexander et al. [2] for the simulation of flows in channels and disk-drive mechanisms respectively. Subsequently, Na-

[1]A significant part of this work has been presented at the 2001 International Mechanical Engineering Congress and Exposition, Heat Transfer Division, session "Fundamentals of Single-Phase Convection"

Contributed by the Heat Transfer Division for publication in the JOURNAL OF HEAT TRANSFER. Manuscript received by the Heat Transfer Division April 6, 2001; revision received August 21, 2001. Associate Editor: J. G. Georgiadis.

gayama et al. [26] investigated heat transfer in channels for Kn >0.001 at a fairly high Mach number (Ma=0.2) using DSMC. Recently, Sun and Faghri [35] investigated the effects of rarefaction and compressibility in flows in two-dimensional channels using DSMC.

In the next section we describe the model problem investigated here. In section 3, we calculate the fully-developed slip-flow Nusselt number in two-dimensional channels in the presence of axial heat conduction. The Nusselt number is found to increase in the presence of axial heat conduction throughout the slip-flow regime; however, the effects of axial heat conduction become less important as the Knudsen number increases. In section 4, we describe the computational model used to extend our calculations to the transition regime; the results obtained using this model are presented and discussed in section 5. In section 5 we also present slip-flow heat transfer results for cylindrical tubes. Those are found to be qualitatively similar to the two-dimensional channel results. We finish with our conclusions.

2 Problem Description

We consider the flow of a gas through a two-dimensional channel of length L with walls that are a distance H apart (see Fig. 1). We denote $T=T(x,y)$ and $P=P(x,y)$ the temperature and pressure fields, respectively. The temperature and pressure at the channel entrance and exit are assumed uniform and denoted (T_i,P_i) and (T_o,P_o), respectively. The gas velocity field is denoted $\vec{\mathbf{u}}=\vec{\mathbf{u}}(x,y)=(u_x(x,y),u_y(x,y),u_z(x,y))$.

The wall temperature is given by

$$T_w(x)=T_i, \quad x<\bar{L}$$

$$T_w(x)=T_o, \quad x\geq\bar{L}.$$

The length $\bar{L}$ is sufficiently large for the flow to develop hydrodynamically before heat transfer between the gas and the wall commences. Similarly, L is sufficiently large for the flow to be thermally fully developed and conditions at the outlet to be uniform. In the next section we derive an expression for the thermal development length. The relative temperature jump was taken to be small, i.e., $|T_o-T_i|/T_i\ll 1$, so that transport coefficients can be assumed constant and acceleration effects small.

As is customary, we define the Reynolds number

$$\mathrm{Re}=\frac{\rho u_b 2H}{\mu}, \tag{1}$$

where μ is the gas viscosity and u_b is the bulk velocity evaluated at the location of interest, the bulk velocity at any station being defined by

$$u_b=\frac{\int_A u_x dA}{\int_A dA}, \tag{2}$$

where A is the cross-sectional area of the channel. The Peclet number is defined as Pe=Re Pr, where Pr is the gas Prandtl number.

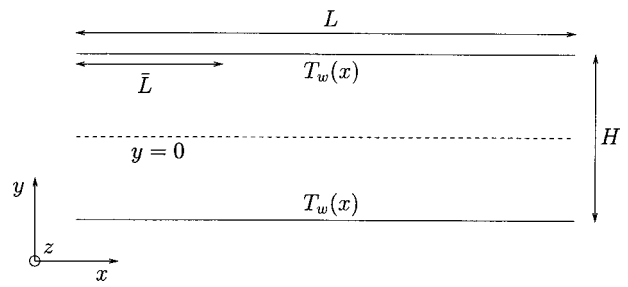

Fig. 1 Channel geometry

A more appropriate measure of the relative importance of convective forces to viscous forces resulting from the fluid acceleration due to compressibility is the modified Reynolds number

$$\mathrm{Re}_L=\frac{\rho u_b 2H}{\mu}\frac{H}{L}. \tag{3}$$

Arkilic et al. [4] have shown that the non-linear pressure distribution measured experimentally can be captured by a ''locally fully developed flow'' model. The effect of fluid acceleration along the channel was considered by Harley et al. [16] who show that for the pressure ratios investigated here, neglecting the fluid acceleration is justified. An alternative approach that is valid throughout the transition regime is discussed in section 5; DSMC simulations show that for $\mathrm{Re}_L<0.1$, the skin friction coefficient equals the fully developed value. Since fluid acceleration directly influences the skin friction coefficient, this is a good indication that ''locally fully developed'' models provide good approximations of the flow physics.

The Nusselt number (non-dimensional heat transfer coefficient h) is defined as

$$\mathrm{Nu}=\frac{h2H}{\kappa}=\frac{q2H}{\kappa(T_w-T_b)}, \tag{4}$$

where κ is the gas thermal conductivity, and T_b is the bulk temperature defined by

$$T_b=\frac{\int_A \rho u_x T dA}{\int_A \rho u_x dA}. \tag{5}$$

Note that in the transition regime linear transport theory is not valid. Although the gas viscosity and thermal conductivity can still be defined, these quantities cease to represent the well-defined transport coefficients associated with linear transport in the continuum regime. They are used here to provide continuity with the already existing continuum frameworks; they also arguably still serve as measures of diffusive transport suitable for use in constructing non-dimensional parameters, especially for Knudsen numbers close to slip flow. Alternatively they can be viewed as the transport coefficients of a reference (unbounded) gas at the temperature of the simulation.

Viscous heat generation can be important in small-scale flows. The (continuum) Brinkman number that quantifies the effect of viscous dissipation is typically defined as

$$\mathrm{Br}^*=\frac{\mu u_b^2}{\kappa(T_w-T_b)}. \tag{6}$$

However, because of the presence of slip, both in temperature and velocity, and because for $\mathrm{Kn}>0.1$ the temperature rise due to dissipation is not correctly captured by the continuum description used to construct the above measure, we constructed a second measure of dissipation; we compare T_w-T_b to the temperature rise due to dissipation in ''isothermal'' $(T_w(x)=T_i)$ simulations at flow velocities equal to the ones encountered in the flows with heat transfer. The modified Brinkman number is defined as

$$\mathrm{Br}=\frac{|T_w-T_b|_{is}}{|T_w-T_b|}, \tag{7}$$

where *is* denotes the ''isothermal'' simulation for the same bulk velocity. In the latter simulations, the flow was gravity driven and periodic, thus avoiding the effects of expansion cooling. As will be discussed below, viscous heat generation will be neglected in the slip-flow analysis and will be very small in our molecular simulations.

The effect of expansion cooling on the temperature field has been investigated by van den Berg et al. [6] for circular capillaries. This work showed that in the continuum regime, the contribution of expansion cooling can also be scaled with the Brinkman number and is of the same order of magnitude as viscous heat

generation. In fact, due to their competing nature, the combined effect of expansion cooling and viscous heat dissipation is smaller than either of the two. DSMC simulations showed that in our molecular results the effects of expansion cooling are expected to be less than 5 percent, and $\mathrm{Br}<0.03$.

3 Slip-Flow Heat Transfer With Axial Heat Conduction

We now present the calculation of the constant-wall-temperature Nusselt number in the slip-flow regime with axial heat conduction. According to slip-fow theory, the gas velocity at the wall differs from the velocity of the wall by an amount that is proportional to the local velocity gradient. The temperature of the gas at the wall is similarly different from the wall temperature by an amount that is proportional to the local temperature gradient. More specifically, for a stationary wall, the velocity slip is given by

$$u_{\mathrm{gas}}|_{\mathrm{wall}}=\alpha\frac{2-\sigma_v}{\sigma_v}\lambda\left.\frac{du}{d\tilde{\eta}}\right|_{\mathrm{wall}}, \tag{8}$$

where σ_v is the momentum accommodation coefficient that is equal to zero for specular reflections and equal to 1 for diffuse reflections [7], and $\tilde{\eta}$ is the coordinate normal to the wall. The thermal slip at the wall is given by a similar expression

$$T_{\mathrm{gas}}|_{\mathrm{wall}}-T_w=\beta\frac{2\gamma}{\gamma+1}\frac{2-\sigma_T}{\sigma_T}\frac{\lambda}{\mathrm{Pr}}\left.\frac{dT}{d\tilde{\eta}}\right|_{\mathrm{wall}}, \tag{9}$$

where σ_T is the energy accommodation coefficient, and γ is the ratio of specific heats.

The coefficients α and β introduce corrections to the original results of Maxwell ($\alpha=\beta=1$) that were obtained through an approximate method [10]. For air, α and β are usually taken to be equal to unity [7]. Hard sphere molecular dynamics simulations, direct Monte Carlo simulations [25,37] and linearized solutions of the Boltzmann equation [23] show that for hard spheres $\alpha\approx\beta\approx1.1$.

The Nusselt number for constant-wall-temperature is obtained by solution of the differential equation governing energy conservation for the system of interest. In the absence of viscous heat generation expansion cooling and transient effects, this equation can be expressed as [24]

$$\rho c_p u_x\frac{\partial T}{\partial x}=\kappa\left(\frac{\partial^2T}{\partial y^2}+\frac{\partial^2T}{\partial x^2}\right), \tag{10}$$

where c_p is the constant pressure heat capacity of the gas. We seek solution of this equation in the region $x\geq\overline{L}$. According to the problem statement in the previous section, the fluid enters the region $x\geq\overline{L}$ at a temperature

$$T=T_i \quad \text{at } x=\overline{L}. \tag{11}$$

The remaining boundary conditions are

$$\frac{\partial T}{\partial y}=0, \quad \text{at } y=0 \tag{12}$$

$$T-T_w=-\beta\frac{2\gamma}{\gamma+1}\frac{2-\sigma_T}{\sigma_T}\frac{\lambda}{\mathrm{Pr}}\frac{\partial T}{\partial y} \quad \text{at } y=\frac{H}{2}, \tag{13}$$

where in the region of interest $x\geq\overline{L}$, $T_w=T_o$.

The velocity distribution in the channel is assumed to be known based on our assumption of hydrodynamically fully developed flow for $x\geq\overline{L}$. It can be written in terms of the bulk velocity u_b as

$$u_x=\frac{u_b}{\mathrm{Kn}+\frac{1}{6}}\left[\left(\mathrm{Kn}+\frac{1}{4}\right)-\frac{y^2}{H^2}\right], \tag{14}$$

or

$$u_\zeta=\frac{3}{2}u_b\frac{1+4\mathrm{Kn}-\eta^2}{1+6\mathrm{Kn}}, \tag{15}$$

where we have used the definitions $\zeta=2(x-\overline{L})/H$ and $\eta=2y/H$ for the axial and transverse non-dimensional coordinates respectively. In the above equation and in what follows, we will absorb α, β, and the accommodation coefficients in the Knudsen number. The origin of the various terms in the final expressions is clear so that these coefficients can be added to the various expressions if desired.

Using the above definitions for the non-dimensional coordinates, the governing differential equation can be written as

$$\mathrm{Pe}\frac{u_\zeta}{4u_b}\frac{\partial\theta}{\partial\zeta}=\frac{\partial^2\theta}{\partial\eta^2}+\frac{\partial^2\theta}{\partial\zeta^2} \tag{16}$$

where $\theta=T-T_w$. Under the assumption of a separable solution of the form

$$\theta=Y(\eta)\exp\left(-\frac{\omega^2}{\mathrm{Pe}}\zeta\right) \tag{17}$$

the original problem is transformed into the following eigenvalue problem

$$\frac{d^2Y}{d\eta^2}+\left(\frac{u_\zeta}{4u_b}+\frac{\omega^2}{\mathrm{Pe}^2}\right)\omega^2Y=0 \tag{18}$$

$$\frac{dY}{d\eta}=0 \quad \text{at } \eta=0 \tag{19}$$

$$Y=-\frac{4\gamma}{\gamma+1}\frac{\mathrm{Kn}}{\mathrm{Pr}}\frac{dY}{d\eta} \quad \text{at } \eta=1 \tag{20}$$

with ω being the corresponding eigenvalue. Solution of this eigevalue problem was obtained through a standard series-solution method [5,34]. More details can be found in [14].

Fully developed conditions correspond to ζ sufficiently large such that only the first eigenvalue ω_0 is important. An approximate criterion for the realization of fully developed conditions can be formulated by requiring that the contribution of the exponential term based on the second eigenvalue (ω_1) is less than 1 percent of the corresponding term based on the first eigenvalue. This can be expressed as

$$\zeta>\zeta_t=\frac{4.6\mathrm{Pe}}{\omega_1^2-\omega_0^2}. \tag{21}$$

This criterion was used to extract the fully developed Nusselt number in our molecular simulations. Note that we will use the superscript s to denote the fully developed Nusselt number calculated using slip-flow theory. We will reserve the symbol Nu_T to denote the Nusselt number for all Kn including the Nusselt number calculated using the molecular simulation technique described in the next section.

Our slip-flow solution neglects the effects of thermal creep that are important in the presence of walls along which a temperature gradient exists. Inman [18] estimates the region in which the effects of thermal creep may be important to be of the order of $0.01\mathrm{Pe}H/2$; based on our results for ω_0 and ω_1, this is much smaller than $\zeta_tH/2$ and hence we expect the effects of thermal creep to be small. This is further discussed in section 5.

4 Transition-Regime Model

Due to the failure of the continuum description in the transition regime, in this section we use a molecular simulation technique to extend our investigation of the constant-wall-temperature heat transfer characteristics beyond slip-flow theory. Molecular modeling will not only provide valuable information about the Nusselt number in the transition regime that very little is known about, but

will also indicate the limits of applicability of slip-flow theory and the rate at which this theory deteriorates in the transition regime.

The molecular simulation technique used here is known as the direct simulation Monte Carlo and in the form used here it models a dilute hard-sphere gas ($\gamma=5/3$, Pr$=2/3$). The properties of a dilute hard-sphere gas are well known, making the connection to the continuum theory of the previous sections fairly straightforward. The viscosity is given by

$$\mu=\frac{5}{16\sigma^2}\sqrt{\frac{mkT}{\pi}},$$

and the thermal conductivity is given by

$$\kappa=\frac{75k}{64\sigma^2}\sqrt{\frac{kT}{\pi m}},$$

where σ is the hard sphere diameter, k is Boltzmann's constant and m is the molecular mass (the gas constant is given by $R=k/m$).

Note that in the constant-wall-temperature problem and its extensions to non-zero Knudsen numbers and non-negligible axial heat conduction, the Nusselt number is independent of the transport coefficients, in the sense that those can be scaled out through proper non-dimensionalization. We thus did not use any collision models that reproduce the temperature variation of transport coefficients of a real monoatomic gas (variable hard sphere, variable soft sphere [9]), since similarity guarantees that our results should be valid for any dilute monoatomic gas in the limit of small temperature changes ($|T_o-T_i|/T_i\ll 1$). To facilitate comparison with our continuum results in which transport coefficients were assumed constant, our molecular results are non-dimensionalized using transport coefficients evaluated at the local gas temperature.

The simulations will exactly follow the problem description given before, and will involve the same assumptions made in the continuum analysis, namely that viscous heat generation and expansion cooling are negligible, transient effects are absent, the flow is fully developed thermally, and that the effect of fluid acceleration is negligible in the dynamics but enters through a ''locally fully developed'' model. The various criteria developed in this paper have been used to ensure that the molecular simulations satisfy these assumptions. In particular, in our simulations Br, $|\mathrm{Br}^*|$, $\mathrm{Re}_L<0.1$; the Nusselt number given in the next section is determined for $\zeta>\zeta_t$. For $\zeta>\zeta_t$ the fluid bulk temperature has typically decayed to within 2 percent of T_w, i.e., $|T_b-T_w|/T_w<0.02$, thus indicating that acceleration effects due to temperature differences should also be small, as assumed in the continuum analysis.

4.1 The Direct Simulation Monte Carlo. The DSMC method [9] is a particle-based stochastic numerical scheme for solving the nonlinear Boltzmann equation [36]. The motion of a representative set of particles is simulated in time in a series of timesteps, each of which involves a ballistic advection of each molecule and stochastic collisions between pairs of molecules. This ''coarse-grained'' molecular description contains the essential physics to fully capture both the hydrodynamic and kinetic regimes [9]. DSMC offers significant modeling advantages compared to continuum techniques in situations where molecular information is required to achieve closure of the governing hydrodynamic equations, or when the continuum hydrodynamic equations are not valid. As with all molecular simulation techniques, macroscopic properties are defined as averages over molecular data. The standard deviation associated with the distribution of the molecular quantities (population standard deviation) determines the uncertainty in our estimation that manifests itself as a noisy signal; this uncertainty is inversely proportional to the square root of the number of samples taken.

For the sake of brevity we will not present a description of the DSMC algorithm. Excellent introductory [1] and detailed [9] descriptions can be found in the literature, as well as comparisons of DSMC simulation results with solutions of the linearized Boltzmann equation [8] for flows in microchannels. Comparisons of DSMC results with experiments for diverse non-equilibrium phenomena spanning the whole Knudsen range can be found in [28,9].

4.2 DSMC Simulations. We simulated gaseous argon ($\sigma=3.66\times10^{-10}$ m, $m=6.63\times10^{-26}$ Kg) at atmospheric density ($\rho=1.78$ Kg/m^3). The hard sphere diameter for argon is well known to reproduce equilibrium and non-equilibrium properties accurately. Gaseous argon has been historically used in a large number of DSMC studies because it provides instant availability to a substantial literature of simulation and experimental results for code validation. This choice should have no effect on our non-dimensionalized results that should apply to any dilute monoatomic gas.

Although continuum calculations can easily be performed for different values of the accommodation coefficients, DSMC simulations are much more computationally expensive and a complete investigation of the full parameter space is beyond our computational capabilities. Additionally, gas-surface interactions for partially accommodating walls are, at present, not well-characterized [9]. We also expect the assumption of full accommodation to be adequate for low speed flows over rough surfaces [9] that are typical of the engineering systems investigated here. This assumption will be relaxed in subsequent studies.

A pressure ratio of $\Pi=P_i/P_o\sim1.4$ is applied at the ends of the channel that causes the gas flow. This pressure ratio balances the conflicting requirements of small velocities for low Mach number and low viscous dissipation, and large velocities for good signal-to-noise ratio. This is particularly important for the calculation of the heat flux at the wall that is the third moment of the molecular velocity distribution function and is very sensitive to noise. The ends of the channels are subject to the inflow and outflow temperatures T_i and T_o respectively, with $\bar{L}=0.2L$. We have found that this satisfies both the hydrodynamic and thermal development criteria.

The heat flux at the wall is defined as the average (over all collisions in a period of time t) energy exchange between the wall and colliding molecules per unit time and area. For hard spheres, only kinetic energy contributes to the energy exchange, and, thus,

$$q=\frac{1}{St}\sum_t\left(\frac{1}{2}m|\vec{V}'|^2-\frac{1}{2}m|\vec{V}|^2\right), \tag{22}$$

where S is the area over which q is defined, t is the period over which averages are taken, $\vec{V}$ is the molecule velocity before collision, and $\vec{V}'$ is the molecule velocity after collision with the wall. Note that the above definition includes the shear work done by the slipping gas at the wall; this contribution should be small in our simulations since it scales with the Brinkman number.

The total number of molecules used (400,000) was such that the average number of molecules per cell was more than 35; that is substantially more than the number (20) empirically determined to be required for accurate solutions. The number of cells was chosen so that the cell linear dimension is at most 0.7 of a mean free path but typically much smaller than that. Alexander et al. [3] have shown that the transport coefficients deviate from the dilute gas Enskog values as the square of the cell size Δx with the proportionality constant such that for cell sizes of the order of one mean free path an error of the order of 10 percent occurs. For $\Delta x\leqslant0.7\lambda$ the difference between the viscosity of the gas and the viscosity of a dilute hard-sphere gas is less than 4.6 percent. We used the results of Alexander et al. [3] to correct all our results for the transport coefficients (viscosity and thermal conductivity).

The timestep of the simulation Δt was taken to be significantly smaller than the mean free time λ/c_o, where $c_o=\sqrt{2RT}$ is the most probable velocity. It has been shown [11,15] that the error in the transport coefficients is proportional to the square of the timestep, with a proportionality constant such that for timesteps of

the order of one mean free time the error is of the order of 5 percent. In our simulations, $\Delta t < \lambda/(7c_o)$, thus making the error negligible.

Due to the impulsive change in wall temperature in the constant-wall-temperature problem, a relatively large signal $(q, T_b - T_w)$ exists; this results in a relatively small uncertainty in the determination of the fully developed Nusselt number, which has additional benefits in terms of driving forces used in the simulation. This is in contrast to the constant-wall-heat-flux case that required large pressure and temperature ratios that resulted in some cases in non-negligible (but small) Brinkman numbers and thermal creep velocities [13].

5 Results and Discussion

5.1 Fully Developed Flow and the Skin Friction Coefficient. In this section we present an expression for the skin friction coefficient

$$C_f = \frac{\tau_w}{(1/2)\rho u_b^2} \tag{23}$$

in fully developed flow that is valid for all Knudsen numbers. This expression is used here to verify the assumption of locally fully developed flow used in our heat transfer calculations.

An expression for the skin friction coefficient in fully developed flow for arbitrary Knudsen numbers can be obtained through the following scaling relation

$$\dot{Q} = u_b H = -\frac{1}{P}\frac{dP}{dx} H^2 \sqrt{\frac{RT}{2}}\,\overline{Q}, \tag{24}$$

which describes the flowrate, $\dot{Q}$, in pressure-driven flow in two-dimensional channels for all Knudsen numbers [10,27]. Here $\overline{Q} = \overline{Q}(\mathrm{Kn})$ has been determined for hard sphere gases by solution of the linearized Boltzmann equation [27,8]. In the absence of fluid acceleration, the pressure gradient must balance the wall shear stress leading to

$$\frac{2\tau_w}{H} = -\frac{dP}{dx}. \tag{25}$$

Combining the above two equations (24,25) leads to

$$C_f = \frac{32}{5\sqrt{\pi}\,\mathrm{Re}\,\mathrm{Kn}\overline{Q}}. \tag{26}$$

Use of a more general viscosity-based mean free path [25] results in an expression that differs by 2 percent.

Figure 2 shows a comparison between Eq. (26) and DSMC simulations in channels with a length to height ratio $L/H = 20$ and fully accommodating walls. The shear stress at the wall is defined and evaluated as the average (over all collisions in a period of time t) momentum exchange between the wall and colliding molecules per unit time and area

$$\tau_w = \frac{m}{St}\sum_t (\vec{V}' \cdot \hat{t} - \vec{V} \cdot \hat{t}), \tag{27}$$

where S is the area over which τ_w is defined, and $\hat{t}$ is the tangent to the wall (positive in the streamwise direction).

The solid line in Figure 2 denotes Eq. (26), the dashed line denotes the slip flow result

$$C_f = \frac{24}{\mathrm{Re}(1 + 6\alpha\mathrm{Kn})} \tag{28}$$

and the stars denote simulation results with error estimates. The bulk velocities in the above simulations where equal to or greater than the corresponding bulk velocities in the calculations with heat transfer. The largest Reynolds number encountered $\mathrm{Re}_L \approx 0.06$ corresponded to the largest channel height H ($\mathrm{Re} \approx 1.2$, $\mathrm{Kn} \approx 0.06$); smaller channel heights were characterized by smaller Reynolds numbers. The agreement between Eq. (26) and simulations is very good and suggests that the flow is well approximated by the locally fully developed assumption.

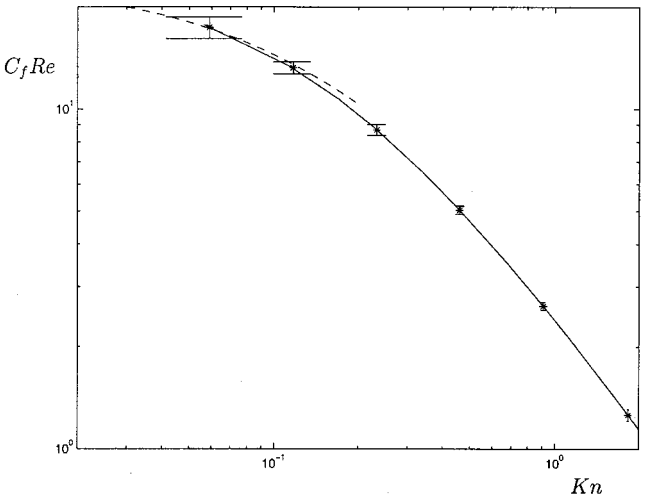

Fig. 2 Comparison between the theoretical prediction of Eq. (26) denoted by a solid line, the slip-flow result (28) with $\alpha = 1.1$ denoted by a dashed line, and the simulation results denoted by stars.

Due to the fairly wide minimum in $\overline{Q}$ centered around $\mathrm{Kn} \approx 1$, equation (26) can be approximated in the region $0.3 < \mathrm{Kn} < 3$ with less than 12 percent error by

$$C_f \approx \frac{2.4}{\mathrm{Kn}\,\mathrm{Re}}. \tag{29}$$

By using the minimum value of $\overline{Q}$ we ensure that Eq. (29) gives an upper bound to the skin friction coefficient in the range $0.3 < \mathrm{Kn} < 3$.

5.2 Slip-Flow Heat Transfer. Figure 3 shows the results of the slip-flow calculation in the range $0 \leq \mathrm{Kn} \leq 0.2$ for air ($\mathrm{Pr} = 0.7$, $\gamma = 1.4$, $\alpha = \beta = 1$) for $\sigma_v = \sigma_T = 1$; we have extended our calcula-

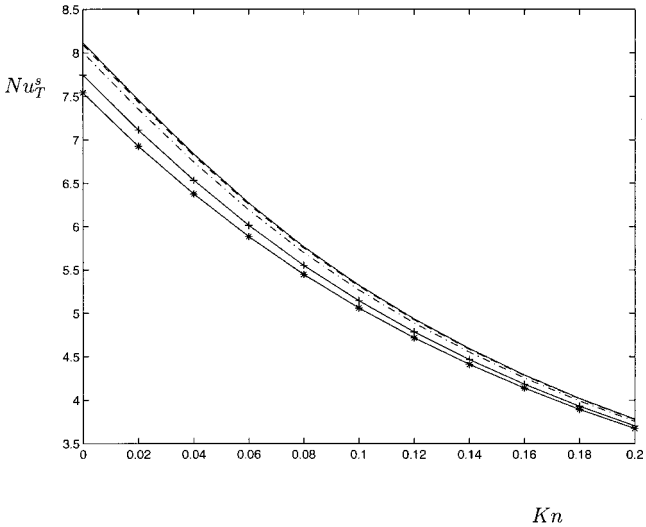

Fig. 3 Variation of Nusselt number Nu_T^s with Knudsen number Kn for air in the fully accommodating case. The solid line denotes Pe→0, the dashed line Pe=0.2, the dash-dotted line Pe=1, the line with crosses Pe=5, and the line with stars Pe→∞.

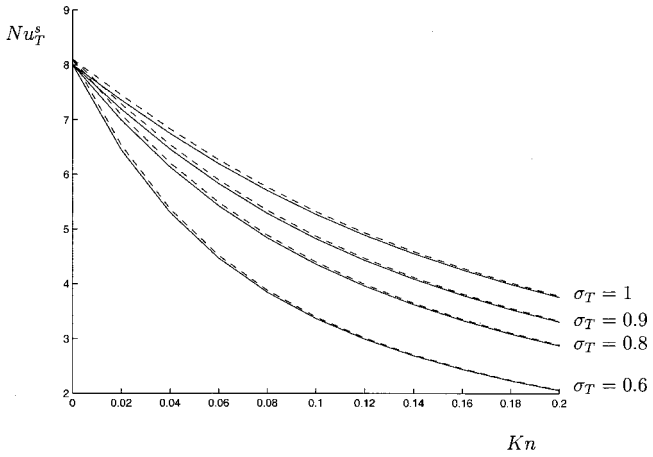

Fig. 4 Variation of Nusselt number Nu_T^s with Knudsen number Kn for air for various values of the thermal accommodation coefficient σ_T with σ_v=1. The solid lines denote Pe=1, and the dashed lines Pe=0.1.

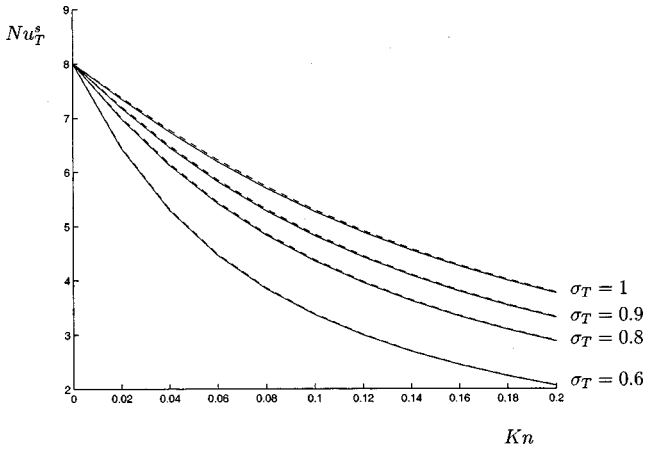

Fig. 5 Variation of Nusselt number Nu_T with Knudsen number Kn for air for various values of the accommodation coefficients for Pe=1. The solid lines denote σ_v=1, and the dashed lines σ_v=0.9.

tions to Kn=0.2 because, as we show later, the slip-flow results are found to be a good approximation to the DSMC results for Kn≤0.2. This figure shows that the Nusselt number decreases monotonically with increasing Knudsen number at constant Pe, for all values of Pe, as expected. The effect of axial heat conduction is to increase the Nusselt number throughout the slip-flow regime. The maximum change occurs at Kn=0 and is of the order of 10 percent, whereas the effects of axial heat conduction are less pronounced as the Knudsen number increases. The dependence of the Nusselt number on the Peclet number in the Pe≪1, Kn=0 limit, is captured by the following asymptotic expression

$$\mathrm{Nu}_T^s(\mathrm{Pe},\mathrm{Kn}=0)=8.11742(1-0.0154295\mathrm{Pe}+0.0017359\mathrm{Pe}^2-\ldots) \quad (30)$$

developed by Grosjean et al. [12], and given here in terms of the Peclet number used in our work.

Although we have presented solutions in the range 0<Pe<∞, the following caveat is in order. Due to the small characteristic dimensions of the channels investigated here, Pe≫1 corresponds to large mean flow velocities that are not consistent with the assumptions of incompressible flow and small Brinkman number made in this study. Hence the solutions for Pe≫1, presented here in the full range 0<Kn<0.2 to facilitate comparison with previous work and illustrate the effects of axial heat conduction, are only physically realistic as Kn→0 and should be interpreted in this way. As we show later, comparison with our DSMC simulations is limited to Pe≤1, since in the latter, Pe≲1.

Figures 4 and 5 show slip-flow results for selected values of the accommodation coefficients. These results show that the dependence of the Nusselt number on the accommodation coefficients is qualitatively similar to the infinite-Peclet number limit studied before [18]: the Nusselt number decreases when the thermal accommodation coefficient decreases; the Nusselt number increases slightly when the momentum accommodation coefficient decreases while the thermal accommodation coefficient remains constant, because a lower momentum accommodation coefficient leads to higher velocities close to the wall and hence enhanced heat transfer. The effect of axial heat conduction is found to be of diminishing importance as the Knudsen number increases, similarly to the fully accommodating case.

The predictions of slip-flow theory for a hard sphere gas (Pr =2/3, γ=5/3, $\alpha=\beta$=1.1) are qualitatively the same. A comparison between the two gases for $\sigma_v=\sigma_T=1$ can be found in Fig. 6.

5.3 Transition-Regime Heat Transfer. Figure 7 shows our DSMC results in the range 0.02<Kn<2 for $\sigma_v=\sigma_T=1$. Simulations with both $T_o>T_i$ and $T_o<T_i$ have been performed. The Peclet number in our simulations was less than 1 (except for Kn =0.029 for which Pe=1.35) that is typical of the small scale flows studied here. This feature also makes the comparison between slip-flow theory and DSMC results easier: due to the diminished importance of axial heat conduction as Kn increases, the dependence of Nusselt number on the Peclet number is very weak. Our slip-flow results show that, in the fully accommodating case, the maximum difference between Nu_T^s(Pe=0.1, 0≤Kn≤0.2) and Nu_T^s(Pe=1, 0≤Kn≤0.2) occurs at Kn=0, and is equal to 1.2 percent. The maximum difference between Nu_T^s(Pe=0.01,0≤Kn ≤0.2) and Nu_T^s(Pe=0.1, 0≤Kn≤0.2) also occurs at Kn=0 as expected, and is less than 0.2 percent. Figure 7 also demonstrates this by comparing the hard-sphere slip-flow results for Pe=0.01, 0.1, and 1.0, which are found to be indistinguishable for Kn>0.1.

Our DSMC results show that in the transition regime the Nusselt number continues to decrease monotonically with increasing Knudsen number when the momentum and thermal accommodation coefficients are equal to unity. The results for Kn<0.1 are in very good agreement with the slip-flow calculation for a hard

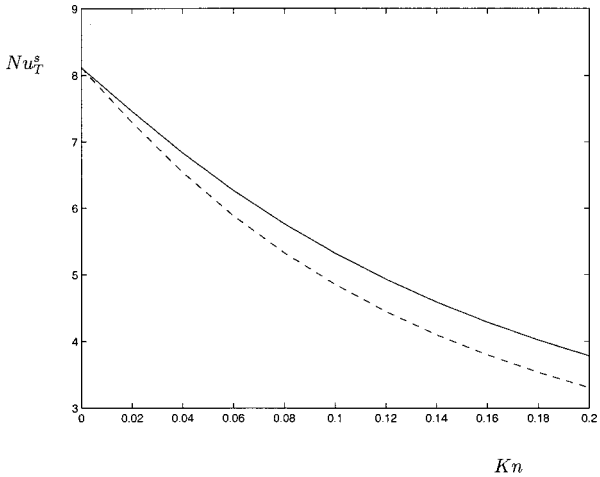

Fig. 6 Variation of Nusselt number Nu_T^s with Knudsen number Kn for Pe→0, $\sigma_v=\sigma_T$=1, for air (solid line) and hard sphere gas (dashed line).

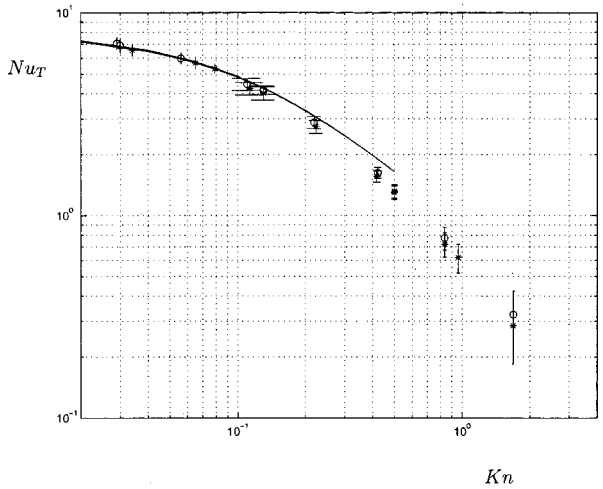

Fig. 7 Variation of Nusselt number Nu_T with Knudsen number Kn. The stars denote DSMC simulation data with $T_o > T_i$ and circles denote DSMC simulation data with $T_i > T_o$. The solid lines denote hard sphere slip-flow results for Pe=0.01, 0.1, and 1.0 which are virtually indistinguishable.

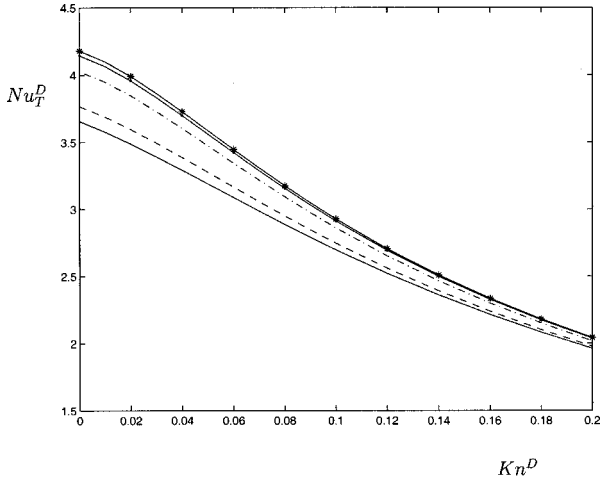

Fig. 8 Variation of Nusselt number Nu_T^D with Knudsen number Kn^D for air in the fully accommodating case. The solid line denotes $Pe^D \to \infty$, the dashed line $Pe^D = 5$, the dash-dotted line $Pe^D = 1$, the line with dots $Pe^D = 0.2$ and the line with stars $Pe^D \to 0$.

sphere gas; as the Knudsen number increases, slip-flow theory overpredicts the Nusselt number. The error (or difference between DSMC and slip-flow theory) is less than 5 percent at Kn≈0.12, and less than 10 percent at Kn≈0.2, indicating that slip-flow theory provides a reasonable approximation beyond Kn=0.1. This is particularly remarkable given that Kn=0.1 corresponds to $Kn' = 0.2$, where $Kn' = \lambda/(H/2)$ is an alternative definition that is frequently used in the literature.

For Kn>0.1, our DSMC results predict that for the same value of the Knudsen number, $Nu_T(T_o > T_i) < Nu_T(T_o < T_i)$. It is possible that this is due to thermal creep flow that provides a ''symmetry breaking'' mechanism since it reverses direction when the temperature gradient along the channel wall reverses direction. Viscous heat generation (including shear work at the boundary) and expansion cooling are also possible sources; they also provide ''symmetry breaking'' mechanisms by introducing a heat flux that is always directed from the fluid to the walls (viscous heat generation) or from the walls to the fluid (expansion cooling), in contrast to the total heat flux that depends on the sign of $T_o - T_i$. As discussed before, the combined effect of viscous heat generation and expansion cooling should be small (Br<0.03), but it is still possible that the *difference* between the two cases (leading to an effect of double magnitude) may be responsible for a discrepancy of the order of 10 percent. The effect is in fact of the order of 5 percent at Kn≈0.4 and increases to approximately 15 percent at Kn≈2. Solution of the continuum equations in the presence of thermal creep is difficult because thermal creep depends on the local axial temperature gradient. However, in the constant-wall-heat-flux case, where the temperature gradient is constant, it is estimated [34] that positive thermal creep ($T_o > T_i$) tends to increase the Nusselt number and negative thermal creep ($T_i > T_o$) decreases the Nusselt number. Here we observe the opposite; however, the above estimate is based on an idealized, plug-flow, thermal creep contribution superimposed on a parabolic (Poiseuille) profile. However, for Kn≫0.1 the velocity profile becomes fairly flat [8]. Additionally, the thermal creep flow profile is steep close to the channel walls in most of the Knudsen regime [22]. This may explain why the opposite trend is observed.

Another possible explanation for the difference between $Nu_T(T_o > T_i)$ and $Nu_T(T_o < T_i)$ is related to the thermal development length that may be longer in the transition regime than the continuum prediction (21). Our DSMC results for Kn>0.4 indicate that the Nusselt number reaches an asymptotic value (within the statistical uncertainty) for $\zeta > 2\zeta_t$ and not $\zeta > \zeta_t$. It is possible that the increased development period is related to thermal creep [33] that decays slowly away from the temperature discontinuity, or due to acceleration effects due to variable fluid temperature despite the fact that at $\zeta = \zeta_t$, $|T_b - T_w|/T_w < 0.02$. Unfortunately, allowing for a larger development length does not resolve this uncertainty because at larger sampling distances than the ones used here, $T_b - T_w$ decays to very small values and the Brinkman number becomes appreciable.

Further work is required to understand the effects of thermal creep and development length and the possible connection between the two. Despite this, our results are still capable of bounding $Nu_T(|T_o - T_i| \to 0)$ to within 15 percent (at most), which is comparable to the statistical uncertainty of these calculations. They also suggest that thermal creep effects in the slip-flow regime are small, thus justifying the neglect of these phenomena in slip-flow analyses.

5.4 Slip-Flow Heat Transfer in Circular Tubes. In this section we present results for slip-flow heat transfer in cylindrical tubes of length L and diameter D. The results presented here include the effects of axial heat conduction that have not been included in previous investigations [5,18,21,34]. The problem description and solution approach is otherwise identical to those in sections 2 and 3 and in the interest of brevity, they will not be included here. More details can be found in [32]. The Reynolds number and Nusselt number for a circular geometry are defined as

$$Re^D = \frac{\rho u_b D}{\mu}, \tag{31}$$

and

$$Nu_T^D = \frac{hD}{\kappa}, \tag{32}$$

respectively. The Knudsen number is defined as $Kn^D = \lambda/D$.

Figure 8 summarizes our results for $Nu_T^D (0 \leqslant Kn^D \leqslant 0.2, 0 < Pe^D < \infty, \sigma_v = \sigma_T = 1)$. In agreement with previous work, for $Kn^D = 0$ the Nusselt number increases as axial heat conduction becomes important (Peclet number decreases). The increase of Nusselt number in the presence of axial heat conduction is less pronounced for non-zero Knudsen numbers: the maximum increase in the Nusselt number occurs at $Kn^D = 0$ and is of the order of 15 percent. In fact, in the regime $Pe^D < 1$ that is of most practical interest, the dependence of Nusselt number on Peclet number

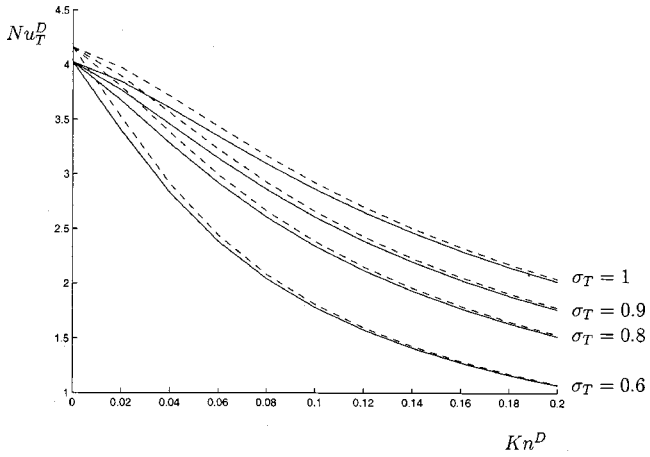

Fig. 9 Variation of Nusselt number Nu_T^D with Knudsen number Kn^D for air for various values of the thermal accommodation coefficient σ_T with σ_v=1. The solid lines denote Pe^D=1, and the dashed lines Pe^D=0.1.

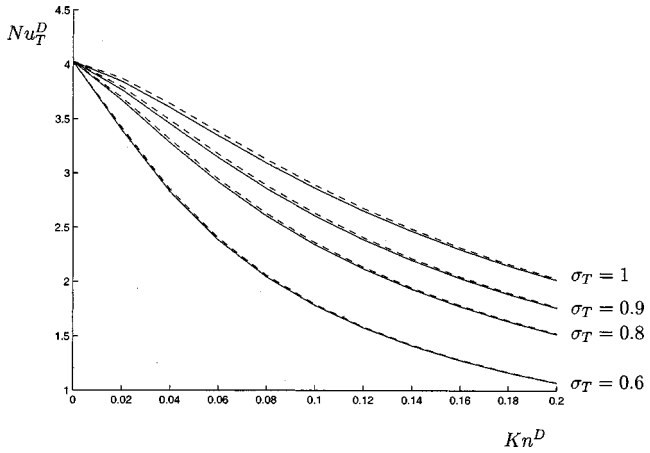

Fig. 10 Variation of Nusselt number Nu_T^D with Knudsen number Kn^D for air for various values of the accommodation coefficients for Pe^D=1. The solid lines denote σ_v=1, and the dashed lines σ_v=0.9.

is weak. The maximum difference between $Nu_T^D(Pe^D=0.2, 0 \leqslant Kn^D \leqslant 0.2)$ and $Nu_T^D(Pe^D=1, 0 \leqslant Kn^D \leqslant 0.2)$ occurs at $Kn^D=0$, and is less than 3 percent. The maximum difference between $Nu_T^D(Pe^D=0.05, 0 \leqslant Kn^D \leqslant 0.2)$ and $Nu_T^D(Pe^D=0.2, 0 \leqslant Kn^D \leqslant 0.2)$ also occurs at $Kn^D=0$ as expected, and is less than 0.7 percent.

Figures 9 and 10 show the variation of the fully developed Nusselt number as a function of Knudsen number for various values of the accommodation coefficients. The qualitative behavior is very similar to the two-dimensional channel case.

6 Conclusions

From the good agreement between the continuum and molecular results in the slip-flow regime and beyond, we conclude that convective heat transfer in low speed flows in the slip-flow regime can be captured by slip-corrected continuum flows that neglect viscous heat dissipation, expansion cooling and thermal creep. The slip coefficients α and β, that are strictly applicable in the presence of a constant gradient in an infinite system, provide good accuracy in channel flows.

The effect of axial heat conduction is to increase the Nusselt number throughout the slip-flow regime. The effect of axial heat conduction decreases as the Knudsen number increases. These findings may explain the weak dependence of Nusselt number on the Reynolds number reported in early experimental work [19].

In the transition regime, the Nusselt number decreases monotonically with increasing Knudsen number for unity momentum and thermal accommodation coefficients. Our transition-regime results, in the non-dimensional form presented here, should be applicable to any dilute monoatomic gas. They are also in qualitative agreement with the previous study that investigated the Nusselt number in the transition regime under constant-wall-heat-flux conditions [13]. The similarity between the Nusselt number and skin friction coefficient dependence on the Knudsen number (see Figs. 2 and 7) suggests that a Reynolds-type analogy may exist. At this time no simple expression for this analogy has been found. The ability of the hard sphere gas model to accurately predict average flow rates of real gases [8] suggests that the skin friction relation (Eq. (26)) should also capture real-gas behavior accurately.

Future work will focus on molecular simulations with accommodation coefficients different from unity. Although our current molecular results suggest that deductions from the slip-flow regime can be qualitatively extended to the transition regime, it would be useful to have exact theoretical predictions. Extensions of this work to polyatomic gases will follow.

Acknowledgments

The authors would like to thank Professors John Lienhard V and Alejandro Garcia for helpful suggestions and discussions, and Professor Triantafyllos Akylas for critically commenting on the manuscript. This work was made possible by the computer resources made available to the authors by the Center for Applied Scientific Computing (CASC) at Lawrence Livermore National Laboratory through the efforts of Dr. Xabier Garaizar. This work was supported in part by Dr. Kyran Mish, Director, Center for Computational Engineering, Lawrence Livermore National Laboratory, U.S. Department of Energy under contract W-7405-ENG-48.

Nomenclature

A = channel cross sectional area (m^2)
Br = modified Brinkman number
Br* = continuum Brinkman number
c_o = most probable (particle) velocity (m/s)
c_p = specific heat at constant pressure (J/Kg K)
c_v = specific heat at constant volume (J/Kg K)
D = tube diameter (m)
H = channel height (m)
h = heat transfer coefficient (W/m^2 K)
Kn = Knudsen number=λ/H
Kn^D = Knudsen number for circular tubes=λ/D
k = Boltzmann's constant (J/K)
L = channel length (m)
$\overline{L}$ = isothermal entry length (m)
m = molecular mass (Kg)
Nu = Nusselt number
Nu_T = constant-wall-temperature Nusselt number
Nu_T^D = constant-wall-temperature Nusselt number for circular tubes
Nu_T^s = slip-flow constant-wall-temperature Nusselt number
P = pressure (Pa)
Pe = Peclet number=RePr
Pe^D = Peclet number for circular tubes=Re^D Pr
P_i = inlet pressure (Pa)
P_o = exit pressure (Pa)
Pr = Prandtl number
$\dot{Q}$ = volume flow rate per unit depth (m^2/s)

$\overline{Q}$ = proportionality constant in volume-flow-rate scaling relation (24)
q = wall heat flux (W/m^2)
R = gas constant=k/m (J/Kg K)
Re = Reynolds number=$\rho u_b 2H/\mu$
Re_L = Re H/L
Re^D = Reynolds number for circular tubes=$\rho u_b D/\mu$
S = flux sampling area (m^2)
T = temperature (K)
T_b = bulk temperature (K)
T_i = inlet temperature (K)
T_o = exit temperature (K)
T_w = wall temperature (K)
t = flux sampling time (s)
$\hat{t}$ = channel wall tangent
$\vec{u}$ = flow velocity (m/s)
u_b = bulk velocity (axial direction) (m/s)
$\vec{V}$ = particle velocity (m/s)
$\vec{V}'$ = post-wall-collision particle velocity (m/s)
x = axial coordinate
y = transverse coordinate
z = out of plane coordinate

Greek Symbols

α = velocity slip coefficient
β = temperature jump coefficient
γ = ratio of specific heats=c_p/c_v
Δx = DSMC cell size (m)
Δt = DSMC timestep (s)
ζ = non-dimensional axial coordinate=$2(x-\overline{L})/H$
ζ_t = non-dimensional thermal development length
η = non-dimensional transverse coordinate=$2y/H$
$\tilde{\eta}$ = coordinate normal to the wall
θ = $T-T_w$ (K)
κ = thermal conductivity (W/m K)
λ = molecular mean free path (m)
μ = coefficient of viscosity (Kg/m s)
Π = pressure ratio=P_i/P_o
ρ = mass density (Kg/m^3)
σ = molecular diameter (m)
σ_T = thermal accommodation coefficient
σ_v = momentum accommodation coefficient
τ_w = wall shear stress (Kg/m s^2)
ω_i = i-th eigenvalue of equation (18)

References

[1] Alexander, F. J., and Garcia, A. L., 1997, "The Direct Simulation Monte Carlo Method," Comput. Phys., **11**, pp. 588–593.
[2] Alexander, F. J., Garcia, A. L., and Alder, B. J., 1994, "Direct Simulation Monte Carlo for Thin-Film Bearings," Phys. Fluids, **6**, pp. 3854–3860.
[3] Alexander, F. J., Garcia, A. L., and Alder, B. J., 1998, "Cell Size Dependence of Transport Coefficients in Stochastic Particle Algorithms," Phys. Fluids, **10**, pp. 1540–1542.
[4] Arkilic, E., Breuer, K. S., and Schmidt, M. A., 1994, "Gaseous Flow FED-197, in Microchannels," *Application of Microfabrication to Fluid Mechanics*, ASME, New York, pp. 57–66.
[5] Barron, R. F., Wang, X., Ameel, T. A., and Washington, R. O., 1997, "The Graetz Problem Extended to Slip-Flow," Int. J. Heat Mass Transf., **40**, pp. 1817–1823.
[6] van den Berg, H. R., Seldam, C. A., and van der Gulik, P. S., 1993, "Thermal Effects in Compressible Viscous Flow in a Capillary," Int. J. Thermophys., **14**, pp. 865–892.
[7] Beskok, A., and Karniadakis, G. E., 1994, "Simulation of Heat and Momentum Transfer in Complex Microgeometries," J. Thermophys. Heat Transfer, **8**, pp. 647–655.
[8] Beskok, A., and Karniadakis, G. E., 1999, "A Model for Flows in Channels and Ducts at Micro and Nano Scales," Microscale Thermophys. Eng., **3**, pp. 43–77.
[9] Bird, G. A., 1994, *Molecular Gas Dynamics and the Direct Simulation of Gas Flows*, Clarendon Press, Oxford.
[10] Cercignani, C., 1988, *The Boltzmann Equation and Its Applications*, Springer-Verlag, New York.
[11] Garcia, A., and Wagner, W., 2000, "Time Step Truncation Error in Direct Simulation Monte Carlo," Phys. Fluids, **12**, pp. 2621–2633.
[12] Grosjean, C. C., Pahor, S., and Strnad, J., 1963, "Heat Transfer in Laminar Flow Through a Gap," Appl. Sci. Res., **11**, pp. 292–294.
[13] Hadjiconstantinou, N. G., 2000, "Convective Heat Transfer in Micro and Nano Channels: Nusselt Number Beyond Slip Flow," *Proceedings of the 2000 IMECE*, HTD-Vol. 366-2, pp. 13–22.
[14] Hadjiconstantinou, N., and Simek, O., 2001, "Nusselt Number in Micro and Nano Channels under Conditions of Constant Wall Temperature," *Proceedings of the 2001 IMECE*.
[15] Hadjiconstantinou, N. G., 2000, "Analysis of Discretization in the Direct Simulation Monte Carlo," Phys. Fluids, **12**, pp. 2634–2638.
[16] Harley, J. C., Huang, Y., Bau, H. H., and Zemel, J. N., 1995, "Gas Flow in Microchannels," J. Fluid Mech., **284**, pp. 257–274.
[17] Ho, C. M., and Tai, Y. C., 1998, "Micro-Electro-Mechanical Systems (MEMS) and Fluid Flows," Annu. Rev. Fluid Mech., **30**, pp. 579–612.
[18] Inman, R. M., 1964, "Heat Transfer for Laminar Slip Flow of a Rarefied Gas in a Parallel Plate Channel or a Circular Tube With Uniform Wall Temperature," NASA TN D-2213.
[19] Kavehpour, H. P., Faghri, M., and Asako, Y., 1997, "Effects of Compressibility and Rarefaction on Gaseous Flows in Microchannels," Numer. Heat Transfer, Part A, **32**, pp. 677–696.
[20] Knudsen, M., 1909, "Die Gesetze der molecular Stromung und dieinneren Reibungstromung der Gase durch Rohren," Annals of Physics, **28**, pp. 75–130.
[21] Larrode, F. E., Housiadas, C., and Drossinos, Y., 2000, "Slip-Flow Heat Transfer in Circular Tubes," Int. J. Heat Mass Transf., **43**, pp. 2669–2690.
[22] Loyalka, S. K., 1975, "Kinetic Theory of Thermal Transpiration and Mechanocaloric Effect. II.," J. Chem. Phys., **63**, pp. 4054–4060.
[23] Loyalka, S. K., 1989, "Temperature Jump and Thermal Creep Slip: Rigid Sphere Gas," Phys. Fluids, **1**, pp. 403–408.
[24] Mills, A. F., 1992, *Heat Transfer*, Irwin.
[25] Morris, D. L., Hannon, L., and Garcia, A. L., 1992, "Slip Length in a Dilute Gas," Phys. Rev. A, **46**, pp. 5279–5281.
[26] Nagayama, K., Farouk, B., and Oh, C. K., 1998, "Heat Transfer in Low Pressure (High Knudsen Number) Developing Flows Through Parallel Plates," *Heat Transfer 1998: Proceedings of the Eleventh International Heat Transfer Conference*, Vol. 3, pp. 127–132.
[27] Ohwada, T., Sone, Y., and Aoki, K., 1989, "Numerical Analysis of the Poiseuille and Thermal Transpiration Flows Between Parallel Plates on the Basis of the Boltzmann Equation for Hard-Sphere Molecules," Phys. Fluids, **1**, pp. 2042–2049.
[28] Oran, E. S., Oh, C. K., and Cybyk, B. Z., 1999, "Direct Simulation Monte Carlo: Recent Advances and Applications," Annu. Rev. Fluid Mech., **30**, pp. 403–431.
[29] Pahor, S., and Strnad, J., 1961, "A Note on Heat Transfer in Laminar Flow Through a Gap," Appl. Sci. Res., **10**, pp. 81–84.
[30] Piekos, E. S., and Breuer, K. S., 1996, "Numerical Modeling of Micromechanical Devices Using the Direct Simulation Monte Carlo Method," ASME J. Fluids Eng., **118**, pp. 464–469.
[31] Shah, R. K., and London, A. L., 1978, *Laminar Flow Forced Convection in Ducts*, Academic Press.
[32] Simek, O., and Hadjiconstantinou, N. G., 2001, "Slip-Flow Constant-Wall-Temperature Nusselt Number in Circular Tubes in the Presence of Axial Heat Conduction," *Proceedings of the 2001 IMECE*.
[33] Sone, Y., 2000, "Flows Induced by Temperature Fields in a Rarefied Gas and Their Ghost Effect on the Behavior of a Gas in Continuum Limit," Annu. Rev. Fluid Mech., **32**, pp. 779–811.
[34] Sparrow, E. M., and Lin, S. H., 1962, "Laminar Heat Transfer in Tubes Under Slip Flow Conditions," ASME J. Heat Transfer, **84**, pp. 363–369.
[35] Sun, H., and Faghri, M., 2000, "Effects of Rarefaction and Compressibility of Gaseous Flow in Microchannel Using DSMC," Numer. Heat Transfer, Part A, **38**, pp. 153–168.
[36] Wagner, W., 1992, "A Convergence Proof for Bird's Direct Simulation Monte Carlo Method for the Boltzmann Equation," J. Stat. Phys., **66**, pp. 1011–1044.
[37] Wijesinghe, S., and Hadjiconstantinou, N. G., 2001, "Velocity Slip and Temperature Jump in Dilute Hard Sphere Gases at Finite Knudsen Numbers," *Proceedings of the First MIT Conference on Computational Fluid and Solid Mechanics*, Vol. 2, pp. 1019–1021.